

# Antiaromaticity and Reactivity of a Planar Cyclooctatetraene Fully Annulated with Bicyclo[2.1.1]hexane Units

Tohru Nishinaga,<sup>\*,[a, c]</sup> Takayuki Uto,<sup>[a]</sup> Ryota Inoue,<sup>[a]</sup> Akira Matsuura,<sup>[a]</sup> Noach Treitel,<sup>[b]</sup> Mordecai Rabinovitz,<sup>[b]</sup> and Koichi Komatsu<sup>\*,[a]</sup>

Dedicated to Professor Klaus Hafner on the occasion of his 80th birthday

**Abstract:** A detailed investigation has been made into the antiaromaticity and chemical reactivity of a planar cyclooctatetraene (COT) molecule fully annulated with bicyclo[2.1.1]hexane units **2**. In spite of its planar  $8\pi$ -electronic structure, theoretical calculations have indicated that the antiaromaticity of COT **2** is considerably decreased in comparison with a planar COT **16** with  $D_{4h}$  symmetry. This behavior appears to be related to the wider HOMO–LUMO gap of **2** relative to **16**, which is caused by the raised LUMO level as a result of the effective  $\sigma$ – $\pi^*$  orbital interaction between the strained bicyclic framework and the COT  $\pi$  system. The

two-electron reduction of **2** required the use of potassium mirror or a combination of lithium/corannulene in highly dried  $[D_8]$ THF at  $-78^\circ\text{C}$  under vacuum. In contrast, the  $[4+2]$  cycloaddition of **2** with tetracyanoethylene (TCNE) proceeded quite smoothly owing to the high-lying HOMO. Reaction of **2** with *meta*-chloroperbenzoic acid gave all-*trans* tetraepoxide **23** in the same way as the corresponding

benzene derivative **3**. While the Simons–Smith-type cyclopropanation of benzene **3** gave tricyclopropanated derivative **21**, the reaction of **2** only afforded isomers of dicyclopropanated derivatives **25** and **26**. Yet, the reactivity of **2** is higher than the parent COT, which does not show any reactivity under the same conditions. On the basis of homodesmotic reactions, it was concluded that release of strain is also an important factor for such relatively high reactivity in the epoxidation and cyclopropanation of bicycloannulated COT **2** as well as benzene **3**.

**Keywords:** antiaromaticity • bicyclo[2.1.1]hexene • cyclooctatetraene • reduction • X-ray diffraction


## Introduction

There has been continued interest in the design and synthesis of planar cyclooctatetraene (COT) derivatives<sup>[1–9]</sup> for the elucidation of antiaromaticity in this typical  $[4n]$   $\pi$ -electron system. Several synthetic and theoretical studies have been carried out<sup>[1–9]</sup> to impose a planar structure on the intrinsically tub-shaped COT ring. However, so far only two derivatives have actualized the complete planarization of a COT ring, except for annulated derivatives with benzene<sup>[1,3,10]</sup> and porphyrin,<sup>[11]</sup> for which the  $\pi$ -conjugative perturbation by aromatic rings precludes precise elucidation of the intrinsic electronic structure of a planar COT ring. The first example is tetrakis(perfluorocyclobuteno)cyclooctatetraene (**1**),<sup>[2]</sup> the structure of which has been determined by X-ray crystallographic studies. COT **1** is characterized by its extraordinarily low reduction potential (i.e.,  $+0.79$  V versus the saturated calomel electrode (SCE);  $+0.33$  V versus the ferrocene (Fc)/ferrocenium ( $\text{Fc}^+$ ) couple)<sup>[2c]</sup> owing to lowering of the

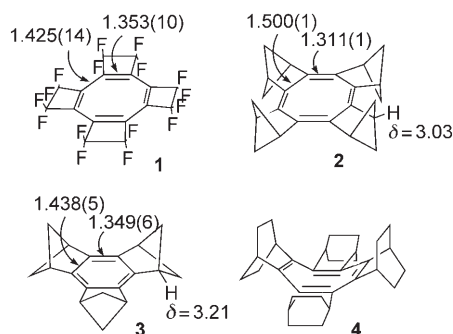
[a] Dr. T. Nishinaga, T. Uto, R. Inoue, Dr. A. Matsuura, Prof. K. Komatsu  
Institute for Chemical Research  
Kyoto University, Uji  
Kyoto 611–0011 (Japan)  
Fax: (+81) 774-38-3178  
E-mail: nishinaga-tohru@tmu.ac.jp  
komatsu@scl.kyoto-u.ac.jp

[b] N. Treitel, Prof. M. Rabinovitz  
Department of Organic Chemistry  
The Hebrew University of Jerusalem  
Givat-Ram, Jerusalem 91904 (Israel)

[c] Dr. T. Nishinaga  
Department of Chemistry  
Graduate School of Science and Engineering  
Tokyo Metropolitan University  
Hachioji, Tokyo 192–0397 (Japan)  
Fax: (+81) 42-677-2525

 Supporting information for this article is available on the WWW under <http://www.chemurj.org/> or from the author.

LUMO level by planarization and the accumulated electron-withdrawing effects of sixteen fluorine atoms. Unfortunately, **1** lacks protons, which are useful for the detection of a paratropic ring current by  $^1\text{H}$  NMR spectroscopic analysis. A recent theoretical study, which employed the continuous transformation of origin of current density (CTOCD) method,<sup>[12]</sup> predicted that a considerable paratropic ring current should be present in **1**,<sup>[13a]</sup> even though the apparent bond alternation in the COT ring was shown by X-ray analysis<sup>[2b]</sup> and theoretical calculations.<sup>[9a,14]</sup>



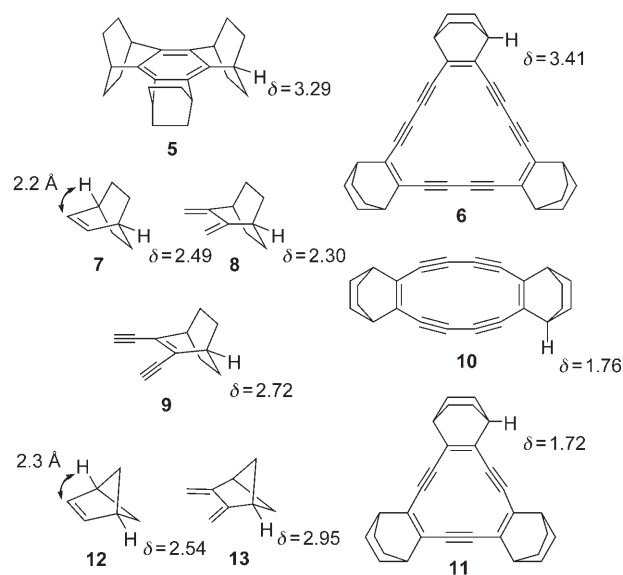
The second example of a planarized COT is a molecule composed of only carbon and hydrogen atoms, tetrakis(bicyclo[2.1.1]hexeno)cyclooctatetraene (**2**), recently synthesized by our group.<sup>[6]</sup> In contrast to **1**, COT **2** showed no reduction in the range 0–2.2 V versus  $\text{Fc}/\text{Fc}^+$  and an unusually low oxidation potential (+0.07 V versus  $\text{Fc}/\text{Fc}^+$ ). This compound, accordingly, gave a fairly stable radical cation salt,<sup>[15]</sup> which is ascribed to a raised HOMO level as a result of the  $\sigma$ - $\pi$  conjugative effects of bicyclic frameworks in addition to a narrowed HOMO–LUMO gap by planarization. The substantial decrease in the HOMO–LUMO gap of the COT ring in **2** is evident from the longest absorption maximum (459 nm),<sup>[6]</sup> remarkably red-shifted relative to that of the tub-shaped tetrakis(bicyclo[2.2.2]octeno)cyclooctatetraene (**4**; 282 nm).<sup>[16]</sup>

The  $^1\text{H}$  NMR chemical shift of the bridgehead proton, which is likely to be a good indicator for the paratropicity of **2** because it is fixed at the same plane as that of the COT ring, showed a surprisingly small upfield shift ( $\Delta\delta = 0.18$  ppm) relative to the signal of the bridgehead proton of tris(bicyclo[2.1.1]hexeno)benzene (**3**).<sup>[6]</sup> Such a small difference may seem to be attributed to a substantial decrease in both the paratropic and diatropic ring currents in **2** and **3**, respectively, as there is a large bond alternation in **2** ( $\Delta R = R_{\text{endo}} - R_{\text{exo}} = 1.500 - 1.331 = 0.169$  Å)<sup>[6]</sup> and **3** ( $\Delta R = 1.438 - 1.349 = 0.089$  Å)<sup>[17]</sup> caused by the annelation with highly strained bicyclo[2.1.1]hexane units. However, calculations of both CTOCD and nucleus-independent chemical shift (NICS)<sup>[18]</sup> demonstrated the presence of considerable amount of antiaromaticity in **2**<sup>[6,13a]</sup> and aromaticity in **3**.<sup>[6,13b]</sup> On the basis of these findings, we decided to examine the antiaromaticity in **2** in detail using observed  $^1\text{H}$  NMR chemical shifts and theoretical calculations. Also, the chemical re-

activity of **2** in two-electron reduction, [4+2] cycloaddition, epoxidation, and cyclopropanation reactions was studied and some of the results were compared with those of the parent COT (and of benzene **3**) to elucidate the effects of aromaticity/antiaromaticity and of the strain of bicyclic frameworks.

## Results and Discussion

**Antiaromaticity of 2:** In our previous study on cyclic  $\pi$ -conjugated systems annelated with bicyclo[2.2.2]octene units, the  $^1\text{H}$  NMR chemical shift of the bridgehead proton was shown to be a good indicator of diatropic or paratropic ring currents.<sup>[19]</sup> For example, the signal of the bridgehead protons in benzene **5** ( $\delta = 3.29$  ppm)<sup>[20]</sup> or aromatic dehydro[18]annulene **6** ( $\delta = 3.41$  ppm)<sup>[21]</sup> are observed downfield shifted by  $\Delta\delta = 0.8$ –1.0 or 0.7 ppm from the signal of the reference compounds, namely, bicyclo[2.2.2]octene (**7**) and 2,3-dimethylenebicyclo[2.2.2]octane (**8**),<sup>[22]</sup> or 2,3-diethynylbicyclo[2.2.2]octene (**9**;  $\delta = 2.49$ , 2.30, and 2.72 ppm, respectively),<sup>[21]</sup> while the resonances of the antiaromatic dehydro[12]annulenes **10** and **11** ( $\delta = 1.76$  and 1.72 ppm, respectively)<sup>[21]</sup> are observed at about  $\Delta\delta = 1$  ppm upfield of the signal for **9**. Since the distances between a

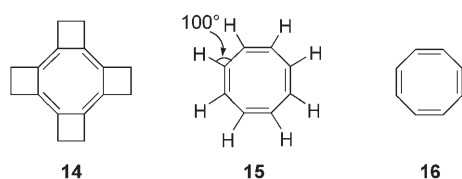


bridgehead proton and the nearest olefinic carbon atoms are almost the same for bicyclo[2.1.1]hexene and bicyclo[2.2.2]octene (ca. 2.3 and 2.2 Å, respectively), the  $^1\text{H}$  NMR chemical shift of the bridgehead proton should reflect the tropicity of the annelated  $\pi$ -conjugated ring to the same extent. In fact, the signal of the bridgehead protons in benzene **3** ( $\delta = 3.21$  ppm)<sup>[6]</sup> showed a downfield shift from that of the reference compounds bicyclo[2.1.1]hexene (**12**)<sup>[23]</sup> or 2,3-dimethylenebicyclo[2.1.1]hexane (**13**;  $\delta = 2.54$  and 2.95 ppm, respectively),<sup>[24]</sup> in a similar extent to the shift ob-

served for benzene **5**. This finding is consistent with the results of the theoretical calculations for the NICS (GIAO-HF/6-31+G(d,p)//B3LYP/6-31G(d)) of **3** (−8.0 ppm), which is large negative value that is rather close to the value of the parent benzene (−9.7 ppm),<sup>[6]</sup> and for the CTOCD method, which indicates the presence of a strong diatropic ring current.<sup>[13b]</sup>

In the case of the planar COT **2**, in spite of the positive NICS value (10.6 ppm)<sup>[6]</sup> and the indication of a paratropic ring current in the CTOCD calculations,<sup>[11a]</sup> the signal of the bridgehead protons ( $\delta = 3.03$  ppm)<sup>[6]</sup> was not shifted upfield but rather slightly downfield in comparison with the signal of reference compound **13**. On the basis of these results, it seems that the antiaromaticity of the planar COT **2** is, if present, substantially decreased in the magnetic criterion. The unexpected downfield shift of the bridgehead proton of **2** would be as a result of a steric compression effect. In the calculated structure of **2** (B3LYP/6-31G(d)), the H...H distance is 2.087 Å, which is shorter than the sum of the van der Waals radius of the hydrogen atom (2.40 Å).

The large bond alternation ( $\Delta R = 0.169(1)$  Å observed by X-ray crystallographic studies;<sup>[6]</sup>  $\Delta R = 0.161$  Å calculated by B3LYP/6-31G(d)) is not the main reason for the considerable decrease in antiaromaticity of **2** since a much larger NICS value (22.1 ppm) was calculated for a hypothetical planar COT unit with exactly the same bond lengths as those in **2**. Calculations for the hypothetical planar COT species, such as **14**, fully annelated with cyclobutane units<sup>[6]</sup>



and **15** with  $D_{4h}$  symmetry and all the C-C-H angles fixed at 100°,<sup>[25]</sup> which have a bond alternation to a similar extent or even larger ( $\Delta R = 0.155$  and 0.18 Å from ref. [6] and B3LYP/6-31G(d) calculations, respectively), also showed large positive NICS values (i.e., 20.9<sup>[6]</sup> and 19.1 ppm). These values are rather closer to the value of the hypothetical planar COT **16** (i.e., 27.2 ppm)<sup>[6]</sup> with a  $D_{4h}$  optimized structure ( $\Delta R = 0.132$  Å; C-C-H angle = 113.9°).

As shown in Figure 1, the planar COT rings have a  $b_{2u}$  HOMO and  $b_{1u}$  LUMO. The  $b_{2u} \rightarrow b_{1u}$  HOMO–LUMO transition has the symmetry of rotation with respect to the direction of the magnetic field and therefore produces a paratropic contribution in the antiaromatic  $\pi$  system.<sup>[13a]</sup> A recent theoretical study showed that this HOMO–LUMO transition dominates the total  $\pi$  ring current in the planar COT and determines its paratropic nature.<sup>[26]</sup> As a result, it can be concluded that the HOMO–LUMO gap is closely related to the strength of paratropicity of the planar COT ring.<sup>[13a]</sup> Thus, the decreased ring current in **2** is ascribed to the larger Kohn–Sham (KS) energy gap between the

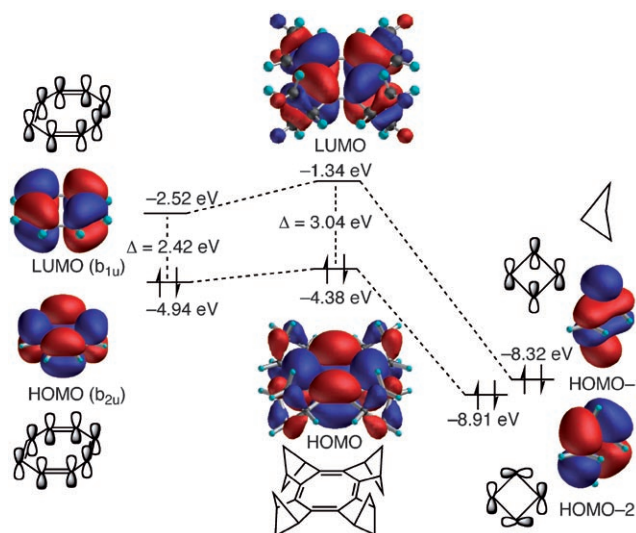
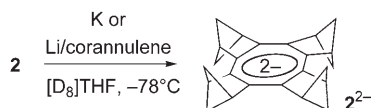


Figure 1. The KS HOMO and LUMO orbitals and their energies calculated at the B3LYP/6-31G(d) level for COT **2** and the imaginary planar COT **16** together with orbital-interaction diagrams between the COT and packed cyclobutane rings of the BCH units.

HOMO and LUMO of **2** (3.04 eV) than the HOMO–LUMO gaps for COTs **14–16** (2.27, 2.75, and 2.42 eV, respectively). Also this tendency is the same for the NICS values of these COTs. The larger HOMO–LUMO gap in COT **2** is mainly ascribed to the relatively high-lying LUMO level of **2** (−1.34 eV) in relation to **14–16** (−2.02, −2.39, and −2.52 eV, respectively). The symmetry of the LUMO of the planar COT **16** ( $b_{1u}$ ) is suitable for mixing with the relatively high-lying HOMO-1 of the cyclobutane moieties of BCH (bicyclo[2.1.1]hexane), and this  $\sigma$ – $\pi^*$  interaction is considered to effectively raise the LUMO level of **2** (Figure 1).

**Two-electron reduction:** Reflecting the elevated LUMO levels of COT **2**, the two-electron reduction of **2** was not so facile relative to the reduction of COT **4**.<sup>[16]</sup> This reaction required highly purified  $[D_8]$ THF as a solvent and proceeded only at −78 °C under vacuum, with either lithium/corannulene<sup>[27]</sup> or with freshly prepared potassium mirror (Scheme 1). The  $^1\text{H}$  and  $^{13}\text{C}$  NMR spectra of the resulting COT dianion **2**<sup>2−</sup> are shown in Figure 2. The signal for the  $\text{sp}^2$  carbon atoms of the COT ring appear at  $\delta = 100.4$  ppm, which is shifted upfield by  $\Delta\delta = 32$  ppm from the signal of neutral **2**, at the almost identical position to the signal ( $\delta = 97.8$  ppm) for the COT dianion annelated with bicyclo[2.2.2]octene **4**<sup>2−</sup>.<sup>[16]</sup> The signals for the CH and  $\text{CH}_2$  moieties of the BCH units are clearly observed at  $\delta = 3.47$ , 2.77, and 1.95 ppm, respectively, thus indicating the quantitative formation of dianion **2**<sup>2−</sup>. The signal for the bridgehead protons ( $\delta = 3.47$  ppm) showed a downfield shift of  $\Delta\delta = 0.44$  ppm from neutral **2**, thus clearly demonstrating the presence of a diatropic ring current in **2**<sup>2−</sup>. In fact, the diatropicity of **2**<sup>2−</sup> was shown by its NICS value of −11.9, which



Scheme 1. Generation of  $2^{2-}$ .

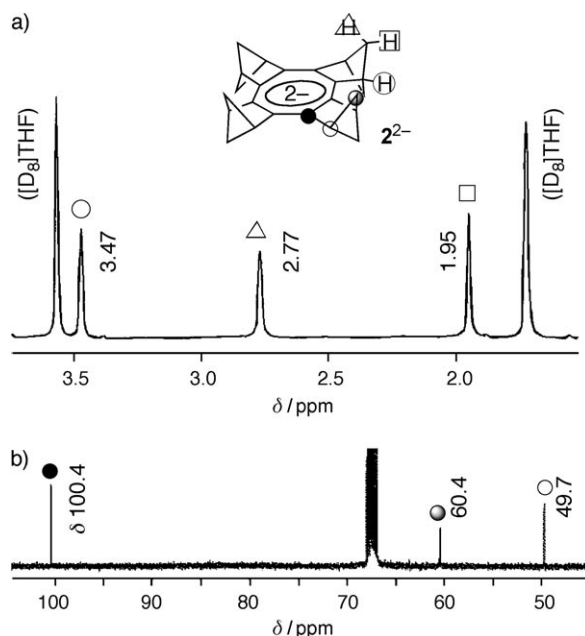


Figure 2. a)  $^1\text{H}$  and b)  $^{13}\text{C}$  NMR spectra of  $2^{2-}$ .

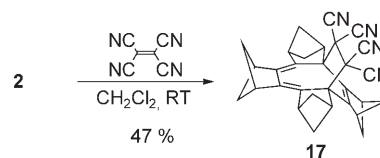
is comparable to the NICS value for the dianion of unsubstituted COT  $16^{2-}$  (i.e.,  $-14.0$  ppm).

Upon the two-electron reduction of **2**, which acquires  $10\pi$ -electron aromaticity, equalization of the bond lengths is expected to take place in the COT ring, and the geometrical influence of annelation with a highly strained bicycloalkene, such as BCH, is of interest.<sup>[9b,28]</sup> As mentioned above,<sup>[29]</sup> such a structural modification causes a large bond alternation in benzene **3**.<sup>[17]</sup> In contrast to **3**, however, the DFT calculations demonstrated that the bond alternation in  $2^{2-}$  is small ( $\Delta R = R_{\text{endo}} - R_{\text{exo}} = 1.431 - 1.405 = 0.026 \text{ \AA}$  as calculated by B3LYP/6-31G(d));  $1.442 - 1.398 = 0.044 \text{ \AA}$  as calculated by B3LYP/6-31+G(d)). This finding is ascribed to the wider inner angle ( $135^\circ$ ) of the eight-membered ring in  $2^{2-}$  than the inner angle ( $120^\circ$ ) of the six-membered ring in **3**. Since the inner angle of  $2^{2-}$  is close to the calculated  $\text{C}=\text{C}-\text{H}$  angle ( $130^\circ$ ) for bicyclo[2.1.1]hexene (**12**), the annelation with BCH groups does not impose much strain and therefore not much bond alternation. For the large bond alternation in **3**, Frank and Siegel suggested the importance of the conjugative effect between the benzene  $\pi$  system and the  $\sigma$  framework of the bicyclo[2.1.1]hexene moiety.<sup>[28]</sup> However, such a conjugative effect appears to be less significant in  $2^{2-}$  judging from the smaller bond alternation.

The higher bond order of the endocyclic bond of the bicyclo[2.1.1]hexene ring in  $2^{2-}$  is also evident from the  $^{13}\text{C}$  NMR spectrum. The  $^{13}\text{C}$  NMR chemical shift of the

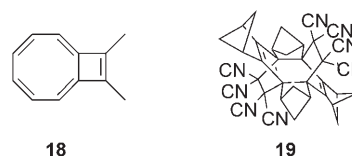
methylene carbon atom of the bicyclo[2.1.1]hexene system is sensitive to the bond order of the endocyclic bond.<sup>[30]</sup> For example, the signal for the methylene carbon atom in bicyclo[2.1.1]hexene (**12**) is observed significantly more downfield ( $\delta = 68.0$  ppm) than the signal for 2,3-dimethylenebicyclo[2.1.1]hexane (**13**;  $\delta = 43.8$  ppm).<sup>[30]</sup> The signal for the methylene carbon atom in the BCH unit of  $2^{2-}$  ( $\delta = 60.4$  ppm, as confirmed by CH COSY spectrum) is also shifted more downfield than the signal for neutral COT **2** ( $\delta = 37.1$  ppm) and even for benzene **3** ( $\delta = 58.4$  ppm). These findings are consistent with the calculated results that more effective bond equalization takes place in the dianion  $2^{2-}$  than in neutral benzene **3**.

**[4+2] Cycloaddition with tetracyanoethylene (TCNE):** Because the HOMO level of COT **2** is considerably elevated as a result of the  $\sigma$ - $\pi$  conjugation, as shown above, the reactivity of **2** as a diene in a cycloaddition reaction should be increased. In fact, when COT **2** was treated with TCNE in dichloromethane at room temperature (Scheme 2), the oc-



Scheme 2. Reaction of **2** with TCNE.

currence of a smooth reaction was apparent from the immediate disappearance of the orange color of **2**, and the [4+2] adduct **17** was isolated in 47% yield. The structure of **17** was determined by X-ray crystallographic studies (Figure 3). The enhanced reactivity of **2** is evident as no reaction took place with the parent COT with TCNE under the same conditions. In spite of the supposed congestion in the transition state, the cycloaddition reaction was quite facile owing to the unusually elevated HOMO level of **2**.<sup>[15]</sup> A similar reaction was also reported to proceed with the nearly planar cyclobuteno derivative **18**,<sup>[31]</sup> which may be better described as a peripheral  $10\pi$ -electron system.



Even in the presence of excess TCNE, further [4+2] cycloaddition of **17** with the second molecule of TCNE did not proceed with heating at  $40^\circ\text{C}$  for 24 h. This behavior is in agreement with the results of the DFT calculations (B3LYP/6-31G(d)), which indicated that the first cycloaddition is moderately endothermic with  $\Delta H = 11.3 \text{ kcal mol}^{-1}$ ,



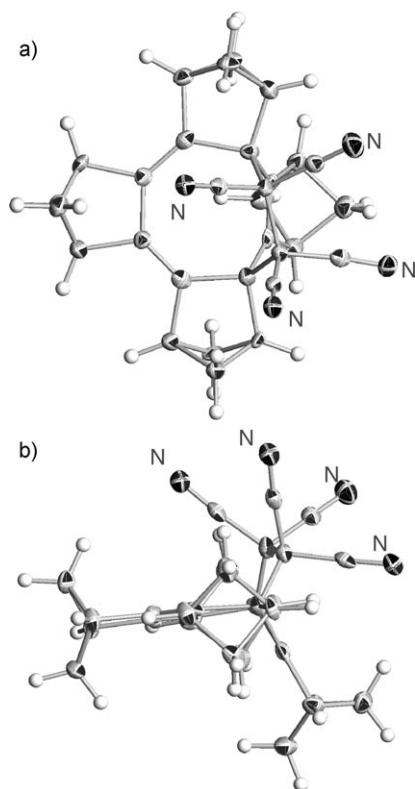
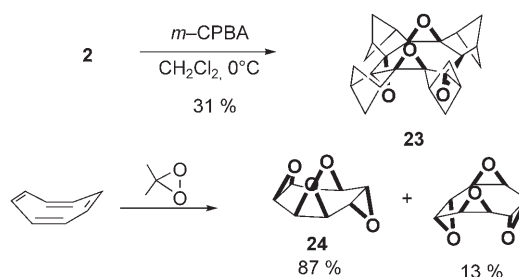
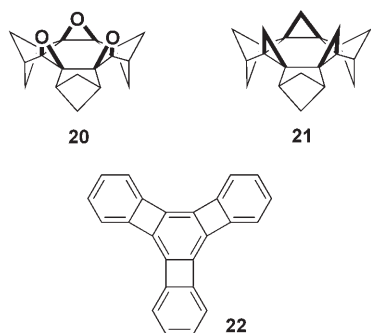


Figure 3. Thermal ellipsoid drawings showing the X-ray structure of **17**. a) Top and b) side views.

while the second cycloaddition requires much higher energy of  $\Delta H = 40.2 \text{ kcal mol}^{-1}$  to produce the unstable adduct **19** with larger steric congestion than **17**.

**Epoxidation and cyclopropanation:** In our previous study, the reactions of benzene **3** with *meta*-chloroperbenzoic acid (*m*-CPBA) in dichloromethane at room temperature and with  $\text{Et}_2\text{Zn}$ /diiodomethane in 1,2-dichloroethane at  $0^\circ\text{C}$  were shown to give all-*cis* tris(epoxide) **20** and all-*cis* tris(cyclopropane) **21** in high yields.<sup>[6]</sup> Similar reactivity was reported for starphenylene **22**.<sup>[32]</sup> Epoxidation and cyclopropanation were attempted for COT **2** under similar conditions to compare the reactivity.

In the case of the epoxidation of **2** (Scheme 3), all four double bonds in **2** were epoxidized within 10 minutes at  $0^\circ\text{C}$



Scheme 3. Comparison of the reactivity of **2** and COT in the epoxidation reaction.

to give tetrakis(epoxide) **23**. Although **23** was detected as a main component in the crude reaction product, the yield of the isolated product was decreased to 31 % as a result of the instability of **23**, which resulted in decomposition during the isolation process. The epoxidation of COT **2**, which has a greater double-bond character than benzene **3**, proceeded faster than for **3** and required a reaction time of 2 hours under the same conditions. However, this behavior is not simply a result of the higher double-bond character of **2** because the reaction of the tub-formed parent COT with *m*-CPBA gives only a mixture of bis(epoxide)s<sup>[33]</sup> and the more reactive dimethyl dioxetane is necessary for complete epoxidation to give tetrakis(epoxide) **24**.<sup>[34]</sup> Thus, the enhanced reactivity of **2** may be partly ascribed to its antiaromatic nature, but “release of strain” could be a more important factor as described below.

The structure of **23** was unambiguously determined by X-ray crystallographic studies. In contrast to the all-*cis* geometry of the tris(epoxide) of benzene **3**, tetrakis(epoxide) **23** has an all-*trans* geometry (Figure 4). To keep the central

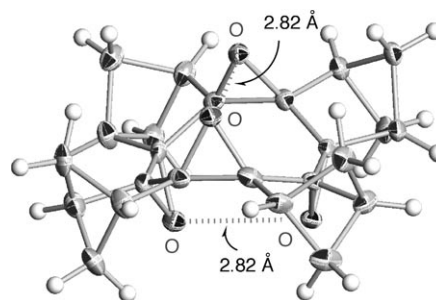
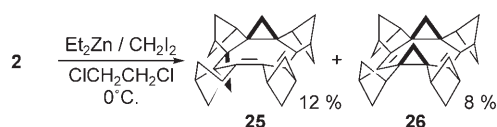


Figure 4. Thermal ellipsoid drawings showing the X-ray structure of **23**.

eight-membered ring in a tub structure holding the four BCH units with the least-strained arrangement, the all-*trans* structure is much more favorable than the all-*cis* structure, thus yielding **23** as a sole product. In the X-ray structure of **23**, the central eight-membered ring is bent like a tub and the distance between the oxygen atoms of the opposite epoxide rings is  $2.82 \text{ Å}$ . This behavior is in contrast to the formation of the tetrakis(epoxide) **24** with *cis-cis-trans* geome-

try in the reaction of the parent COT with dimethyl dioxetane.

Next, the Simons–Smith-type cyclopropanation was attempted with COT **2** at room temperature (Scheme 4). In



Scheme 4. Cyclopropanation of **2**.

contrast to the complete all-*cis* cyclopropanation of benzene **3**,<sup>[6]</sup> only two of the four double bonds were transformed into cyclopropane rings to afford two isomers of bis(cyclopropane) products **25** and **26**. Again, the enhanced reactivity of COT **2** in relation to the parent COT is apparent because the parent COT shows no reactivity at all under the same conditions. Further cyclopropanation of **25** or **26** did not proceed, even at  $60^\circ\text{C}$  for 2 h with additional cyclopropanation reagents.

The precise structures of **25** and **26** were determined by X-ray crystallographic studies (Figure 5). The orientation of the cyclopropane rings is *trans* for the adjacently cyclopropanated product **25** and *cis* for the oppositely cyclopropanated product **26**. This tendency is consistent with the epoxidation of **2**, thus supporting the idea that the reactions are controlled by product stability.

In the X-ray structure of *cis*-cyclopropanated **26**, the distance between the methylene carbon atoms of the cyclopropane rings is  $3.49 \text{ \AA}$ , which is apparently longer than the distance between the oxygen atoms in **23** as a result of the

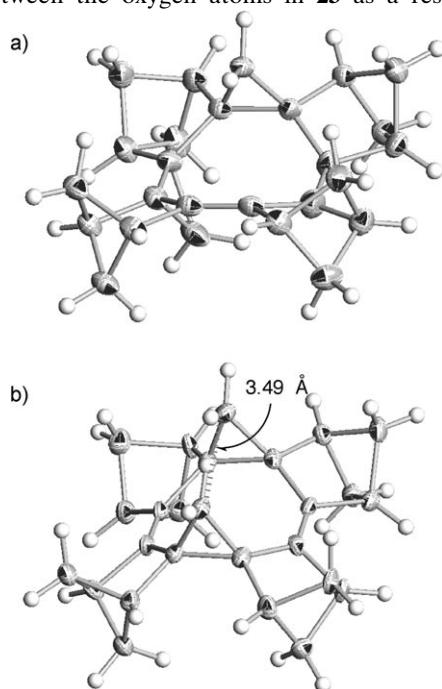
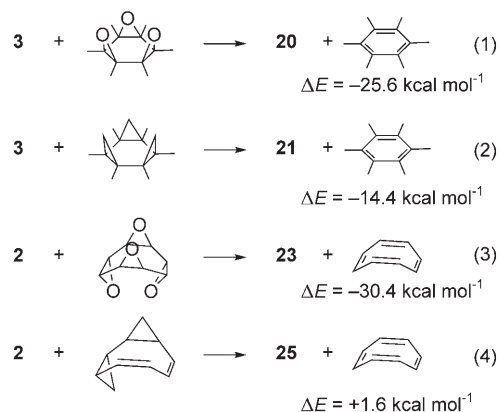


Figure 5. Thermal ellipsoid drawings showing the X-ray structure of a) **25** and b) **26**.

steric repulsion between the methylene hydrogen atoms. This repulsion causes shallower folding in the tub structure of **26**. Consequently, tris- and tetrakis(cyclopropane) derivatives of **2** should have greater strain than the corresponding epoxides, which could be the reason for no higher cyclopropanated products being formed.

To examine the effect of strain by annelation with BCH units, the energetics for homodesmotic reactions (1)–(4) were calculated using the DFT method. In the case of the ben-



zene derivatives, both reactions (1) and (2) are highly exothermic, which is consistent with the preferable formation of **20** and **21**. Since the aromatic stabilization energy of **3** is comparable to that of the parent benzene, despite its cyclohexatriene-like geometry,<sup>[6]</sup> the exothermicity principally derives from the release of strain in the bicyclic systems in **3** by transformation into **20** and **21**, in which the endocyclic bonds become longer by saturation. Due to the same reason, reaction (3) is also highly exothermic, whereas reaction (4) is slightly endothermic in agreement with the experimental results. Thus, irrespective of aromaticity and antiaromaticity, the release of strain appears to be the principal driving force for the epoxidation and cyclopropanation of benzene **3** and COT **2**.

## Conclusion

In summary, we have surveyed the antiaromaticity of the planar COT **2** on the basis of the results of NMR spectroscopic analysis and theoretical calculations and also clarified the chemical reactivity of **2** including two-electron reduction,  $[4+2]$  cycloaddition, epoxidation, and cyclopropanation reactions. In spite of the planar  $8\pi$ -electronic system, the antiaromaticity of **2** is considerably decreased with respect to the hypothetical planar COT **16**. This behavior is ascribed to an effective  $\sigma$ - $\pi^*$  orbital interaction between the bicyclic  $\sigma$  framework and the COT  $\pi$  system. The HOMO–LUMO gap in COT **2** is small for an  $8\pi$ -electron system, as judged from its orange color and the long-wavelength absorption. Thus, two-electron reduction proceeds under care-

fully controlled conditions, and the [4+2] cycloaddition with TCNE readily takes place owing to the high-lying HOMO. Concerning the epoxidation reaction, COT **2** and benzene **3** were shown to have similar reactivities. However, in the case of cyclopropanation, the reactivity of **2** was unexpectedly lower than **3**. From the results of these experiments and theoretical calculations, it can be concluded that the release of strain is an important driving force for epoxidation and cyclopropanation irrespective of the antiaromaticity of **2** or aromaticity of **3**.

## Experimental Section

**General procedures:** Chemical shifts of the  $^1\text{H}$  and  $^{13}\text{C}$  NMR spectra (300 and 75.4 MHz, respectively) are reported in ppm with reference to tetramethylsilane with the signal of the solvents as the internal standard ( $\delta = 7.26$ , 5.32, and 3.57 for  $\text{CHCl}_3$ ,  $\text{CH}_2\text{Cl}_2$ , and  $[\text{D}_8]\text{THF}$ , respectively, in the  $^1\text{H}$  NMR spectra and  $\delta = 77.0$ , 54.0, and 67.39 ppm in the  $^{13}\text{C}$  NMR spectra for  $\text{CDCl}_3$ ,  $\text{CD}_2\text{Cl}_2$ , and  $[\text{D}_8]\text{THF}$ , respectively). Preparative gel-permeation chromatography (GPC) was performed with a JAI LC-908 chromatograph equipped with JAIGEL 1H and 2H columns. All the reactions were carried out under argon unless otherwise noted. THF, diethyl ether, and toluene were distilled from sodium benzophenone ketyl. Dichloromethane, hexane, and *N,N*-dimethylformamide (DMF) were distilled over  $\text{CaH}_2$ ; ethanol was distilled over  $\text{K}_2\text{CO}_3$ ; and 1,2-dichloroethane and  $\text{CS}_2$  were distilled over  $\text{P}_2\text{O}_5$ . TCNE was purified by sublimation under reduced pressure and *meta*-chloroperbenzoic acid (*m*-CPBA) was purified by treatment with aqueous  $\text{NaH}_2\text{PO}_4/\text{NaOH}$  ( $\text{pH} \approx 7.4$ ). COT **2** and benzene **3** were synthesized as reported previously.<sup>[6]</sup> All the other commercially available materials were of reagent grade unless otherwise noted.

**Computational method:** All the calculations were conducted using Gaussian 98 programs.<sup>[35]</sup> The geometries were optimized with the restricted Becke hybrid (B3LYP) at the 6-31G(d) level, and the magnetic properties were calculated using the GIAO method at the HF/6-31+G(d,p) level. For comparison, the geometry of **2**<sup>2-</sup> was also optimized with diffuse functions, namely, 6-31+G(d).

**Two-electron reduction of COT 2:** COT **2** was reduced in 5-mm NMR glass tubes equipped with an upper reduction chamber. The COT (3–5 mg) was introduced into the lower chamber of the tube under argon. The alkali metal (kept in paraffin oil, cleansed from the oxidized layer, and rinsed in petroleum ether 40–60°C) was introduced under argon to the reduction chamber as a lithium wire or piece of potassium. The tube was then placed under high vacuum and dried by flame. In the case of lithium, a catalytic amount of corannulene was added to promote electron transfer. In the case of potassium, the metal was sublimed several times, thus creating a potassium mirror on the reduction chamber. Approximately 1 mL of anhydrous  $[\text{D}_8]\text{THF}$  (dried over a sodium/potassium alloy under high vacuum) was vacuum transferred to the NMR tube and was degassed several times. Finally, the tube was flame-sealed under high vacuum:  $^1\text{H}$  NMR ( $[\text{D}_8]\text{THF}$ ):  $\delta = 3.47$  (m, 4H), 2.77 (m, 8H), 1.95 (m, 8H) ppm;  $^{13}\text{C}$  NMR ( $[\text{D}_8]\text{THF}$ ):  $\delta = 100.41$ , 60.42, 49.72 ppm.

**[4+2] Cycloaddition of COT 2 with TCNE:** COT **2** (12.1 mg, 0.0387 mmol) and TCNE (5.60 mg, 0.0448 mmol) were dissolved in  $\text{CH}_2\text{Cl}_2$  (16 mL). After stirring for 5 min at room temperature, the solvent was evaporated under reduced pressure. Separation of the residue by GPC eluting with  $\text{CHCl}_3$  afforded **17** (8.0 mg, 47%) as a colorless solid. The substance gradually darkened above 120°C but did not melt below 300°C.  $^1\text{H}$  NMR ( $\text{CDCl}_3$ ):  $\delta = 3.23$  (dt,  $J = 6.9$ , 2.9 Hz, 2H), 3.20–3.12 (m, 4H), 3.01 (dd,  $J = 9.9$ , 3.3 Hz, 1H), 2.77 (t,  $J = 2.3$  Hz, 2H), 2.72 (dt,  $J = 5.4$ , 2.4 Hz, 1H), 2.67 (dt,  $J = 6.0$ , 2.4 Hz, 1H), 2.47 (dd,  $J = 10.8$ , 8.4 Hz, 2H), 2.36 (dd,  $J = 9.9$ , 5.3 Hz, 1H), 2.16–2.04 (m, 6H), 1.86 (dd,  $J = 9.9$ , 6.3 Hz, 1H), 1.46 (dd,  $J = 10.4$ , 7.0 Hz, 2H), 1.32 (dd,  $J = 9.8$ , 6.2 Hz, 1H) ppm;  $^{13}\text{C}$  NMR ( $\text{CDCl}_3$ ):  $\delta = 151.2$ , 137.6, 136.6, 113.5, 112.7,

66.7, 63.6, 54.4, 54.0, 48.8, 47.8, 46.4, 45.8, 45.0, 43.0, 42.9, 36.2 ppm; EI-MS:  $m/z$ : 440.3 [ $M^+$ ]; HR-MS calcd (%) for  $\text{C}_{30}\text{H}_{24}\text{N}_4$ : 440.2001; found: 440.2010.

**Epoxidation of COT 2:** A solution of *m*-CPBA (75 mg of 80% pure reagent; 60 mg, 0.430 mmol) in  $\text{CH}_2\text{Cl}_2$  (0.7 mL) was added dropwise to a stirred solution of COT **2** (16.8 mg, 0.0538 mmol) in  $\text{CH}_2\text{Cl}_2$  (10 mL) at 0°C. After stirring for 5 min, the reaction mixture was quenched by addition of saturated aqueous  $\text{NaHCO}_3$ . The organic layer was separated, and the aqueous layer was extracted with  $\text{CH}_2\text{Cl}_2$  (2  $\times$  5 mL). The combined organic phase was dried over  $\text{MgSO}_4$ . The solvent was removed under reduced pressure and the residue was subjected to flash chromatography on alumina eluting with  $\text{CH}_2\text{Cl}_2$  to give tetraepoxide **23** (6.3 mg, 31%) as a colorless solid. The substance gradually darkened above 180°C and exploded at 200°C.  $^1\text{H}$  NMR ( $\text{CDCl}_3$ ):  $\delta = 2.25$  (t,  $J = 2.7$  Hz, 8H), 2.04 (sex,  $J = 2.6$  Hz, 8H), 1.89 (dd,  $J = 5.0$ , 2.3 Hz, 8H) ppm;  $^{13}\text{C}$  NMR ( $\text{CDCl}_3$ ):  $\delta = 75.7$ , 44.2, 37.7 ppm; APCI-MS:  $m/z$ : 376.4 [ $M^+$ ]; HR-MS (FAB) calcd (%) for  $\text{C}_{24}\text{H}_{25}\text{O}_4$ : 377.1753; found: 377.1754.

**Cyclopropanation of COT 2:**  $\text{Et}_2\text{Zn}$  (0.70 mL, 0.71 mmol; 1.02 M in hexane) was added dropwise to a stirred solution of COT **2** (23.9 mg, 0.0765 mmol) in 1,2-dichloroethane (10 mL) at 0°C. After stirring for 5 min,  $\text{CH}_2\text{I}_2$  (0.10 mL, 1.30 mmol) was added. After stirring for 15 min, the reaction mixture was quenched by addition of saturated aqueous  $\text{NH}_4\text{Cl}$  and the reaction mixture was allowed to warm to room temperature. The organic layer was separated, and the aqueous layer was extracted with  $\text{CH}_2\text{Cl}_2$  (2  $\times$  5 mL). The combined organic solution was dried over  $\text{MgSO}_4$ . Removal of the solvent and GPC separation of the residue eluting with  $\text{CHCl}_3$  gave **25** (3.1 mg, 12%) and **26** (2.0 mg, 8%) as colorless solids. **25**: m.p. 192–193°C;  $^1\text{H}$  NMR ( $\text{CDCl}_3$ ):  $\delta = 3.32$  (dt,  $J = 7.8$ , 2.7 Hz, 2H), 3.05 (t,  $J = 2.7$  Hz, 2H), 2.16 (dt,  $J = 7.5$ , 2.7 Hz, 2H), 2.14 (t,  $J = 2.8$  Hz, 2H), 2.00–1.95 (m, 4H), 1.93 (dt,  $J = 6.0$ , 2.6 Hz, 2H), 1.85–1.77 (m, 4H), 1.62 (dd,  $J = 3.6$ , 1.8 Hz, 2H), 1.40–1.32 (m, 2H), –0.04 ppm (d,  $J = 3.6$  Hz, 2H);  $^{13}\text{C}$  NMR ( $\text{CDCl}_3$ ):  $\delta = 136.2$ , 109.2, 48.9, 48.1, 46.6, 45.7, 43.9, 41.9, 41.7, 41.5, 40.6, 38.2, 15.0 ppm; EI-MS:  $m/z$ : 340 [ $M^+$ ]; HR-MS: calcd (%) for  $\text{C}_{26}\text{H}_{28}$ : 340.2191; found: 340.2194. **26**: gradually decomposed above 180°C;  $^1\text{H}$  NMR ( $\text{CDCl}_3$ ):  $\delta = 3.23$  (dt,  $J = 7.8$ , 2.9 Hz, 4H), 2.01 (dt,  $J = 8.1$ , 2.7 Hz, 4H), 1.80 (sex,  $J = 2.8$  Hz, 8H), 1.46 (t,  $J = 2.4$  Hz, 8H), 1.25 (s, 2H), 0.78 (d,  $J = 7.8$  Hz, 2H) ppm;  $^{13}\text{C}$  NMR ( $\text{CDCl}_3$ ):  $\delta = 133.9$ , 50.1, 46.3, 43.0, 42.1, 41.5, 26.6 ppm; EI-MS:  $m/z$ : 340 [ $M^+$ ]; HR-MS calcd (%) for  $\text{C}_{26}\text{H}_{28}$ : 340.2191; found: 340.2191.

**X-ray structural analysis:** Intensity data were collected at 100 K on a Bruker SMART APEX diffractometer with  $\text{MoK}_\alpha$  radiation ( $\lambda = 0.71073$  Å) and graphite monochromator. The structure was solved by direct methods (SHELXTL) and refined by the full-matrix least-squares on  $F^2$  (SHELXL-97). All the non-hydrogen atoms were refined anisotropically and all the hydrogen atoms were placed using AFIX instructions.

**17:** Single crystals suitable for X-ray crystallography were obtained by recrystallization from  $\text{CH}_2\text{Cl}_2$ /hexane.  $\text{C}_{30}\text{H}_{24}\text{N}_4$ ,  $M_w = 440.53$ , crystal size =  $0.10 \times 0.10 \times 0.04$  mm<sup>3</sup>, monoclinic,  $P2(1)$ ,  $a = 9.614(5)$ ,  $b = 12.224(5)$ ,  $c = 10.342(5)$  Å,  $\beta = 115.658(2)^\circ$ ,  $V = 1095.6(9)$  Å<sup>3</sup>,  $Z = 2$ ,  $\rho_{\text{calcd}} = 1.335$  g cm<sup>–3</sup>; the refinement converged to  $R_1 = 0.0523$ ,  $wR_2 = 0.0789$  ( $I > 2\sigma(I)$ ), GOF = 1.004.<sup>[36]</sup>

**23:** Single crystals suitable for X-ray crystallography were obtained by recrystallization from  $\text{CH}_2\text{Cl}_2$ .  $\text{C}_{24}\text{H}_{24}\text{O}_4$ ,  $M_w = 376.43$ , crystal size =  $0.20 \times 0.20 \times 0.20$  mm<sup>3</sup>, monoclinic,  $P2(1)/n$ ,  $a = 11.137(5)$ ,  $b = 12.193(5)$ ,  $c = 13.343(5)$  Å,  $\beta = 90.344(5)^\circ$ ,  $V = 1811.9(13)$  Å<sup>3</sup>,  $Z = 4$ ,  $\rho_{\text{calcd}} = 1.380$  g cm<sup>–3</sup>; the refinement converged to  $R_1 = 0.1061$ ,  $wR_2 = 0.2225$  ( $I > 2\sigma(I)$ ), GOF = 1.183.<sup>[36]</sup>

**25:** Single crystals suitable for X-ray crystallography were obtained by recrystallization from  $\text{CH}_2\text{Cl}_2$ /hexane. One of methylene carbon atoms of the cyclopropane moieties is disordered and the occupancies of the disordered atoms were refined as 0.79:0.21.  $\text{C}_{26}\text{H}_{28}$ ,  $M_w = 340.48$ , crystal size =  $0.10 \times 0.10 \times 0.10$  mm<sup>3</sup>, monoclinic,  $P2(1)/n$ ,  $a = 10.613(5)$ ,  $b = 12.021(5)$ ,  $c = 14.337(5)$  Å,  $\beta = 96.423(5)^\circ$ ,  $V = 1817.6(13)$  Å<sup>3</sup>,  $Z = 4$ ,  $\rho_{\text{calcd}} = 1.244$  g cm<sup>–3</sup>; the refinement converged to  $R_1 = 0.0463$ ,  $wR_2 = 0.0842$  ( $I > 2\sigma(I)$ ), GOF = 1.003.<sup>[36]</sup>

**26:** Single crystals suitable for X-ray crystallography were obtained by recrystallization from  $\text{CH}_2\text{Cl}_2$ /hexane.  $(\text{C}_{26}\text{H}_{28})_2$ ,  $M_w = 680.97$ , crystal size =

$0.10 \times 0.10 \times 0.05 \text{ nm}^3$ , triclinic,  $P\bar{1}$ ,  $a = 9.338(5)$ ,  $b = 11.000(5)$ ,  $c = 17.671(5) \text{ \AA}$ ,  $\alpha = 85.489(5)^\circ$ ,  $\beta = 85.009(5)^\circ$ ,  $\gamma = 89.248(5)^\circ$ ,  $V = 1802.6(14) \text{ \AA}^3$ ,  $Z = 2$ ,  $\rho_{\text{calcd}} = 1.255 \text{ g cm}^{-3}$ ; the refinement converged to  $R_1 = 0.0645$ ,  $wR_2 = 0.1418$  ( $I > 2\sigma(I)$ ), GOF = 1.001.<sup>[36]</sup>

## Acknowledgement

This study was supported by a Grant-in-Aid for Scientific Research (B) (No. 14340196) from the Ministry of Education, Culture, Sports, Science and Technology, Japan.

- [1] C. F. Wilcox, Jr., J. P. Uetrecht, K. K. Grohman, *J. Am. Chem. Soc.* **1972**, *94*, 2532.
- [2] a) R. L. Soulen, S. K. Choi, J. D. Park, *J. Fluorine Chem.* **1973/74**, *3*, 141; b) F. W. B. Einstein, A. C. Willis, W. R. Cullen, R. L. Soulen, *J. Chem. Soc. Chem. Commun.* **1981**, 526; c) W. E. Britton, J. P. Ferraris, R. L. Soulen, *J. Am. Chem. Soc.* **1982**, *104*, 5322.
- [3] I. Willner, M. Rabinovitz, *J. Org. Chem.* **1980**, *45*, 1628.
- [4] M. C. Pirrung, N. Krishnamurthy, D. S. Nunn, A. T. McPhail, *J. Am. Chem. Soc.* **1991**, *113*, 4910.
- [5] F.-G. Klärner, R. Ehrhardt, H. Bandmann, R. Boese, D. Blaser, K. N. Houk, B. R. Beno, *Chem. Eur. J.* **1999**, *5*, 2119.
- [6] A. Matsuura, K. Komatsu, *J. Am. Chem. Soc.* **2001**, *123*, 1768.
- [7] O. Ermer, F.-G. Klärner, M. J. Wette, *J. Am. Chem. Soc.* **1986**, *108*, 4908.
- [8] C. Trindle, T. Wolfskill, *J. Org. Chem.* **1991**, *56*, 5426.
- [9] a) K. K. Baldridge, J. S. Siegel, *J. Am. Chem. Soc.* **2001**, *123*, 1755; b) K. K. Baldridge, J. S. Siegel, *J. Am. Chem. Soc.* **2002**, *124*, 5514.
- [10] D. Hellwinkel, G. Reiff, *Angew. Chem.* **1970**, *82*, 516; *Angew. Chem. Int. Ed. Engl.* **1970**, *9*, 527.
- [11] a) Y. Nakamura, N. Aratani, H. Shinokubo, A. Takagi, T. Kawai, T. Matsumoto, Z. S. Yoon, D. Y. Kim, T. K. Ahn, D. Kim, A. Muranaka, N. Kobayashi, A. Osuka, *J. Am. Chem. Soc.* **2006**, *128*, 4119; b) S. Hiroto, K. Furukawa, H. Shinokubo, A. Osuka, *J. Am. Chem. Soc.* **2006**, *128*, 12380.
- [12] T. A. Keith, R. F. W. Bader, *Chem. Phys. Lett.* **1993**, *210*, 223.
- [13] a) P. W. Fowler, R. W. A. Havenith, L. W. Jenneskens, A. Soncini, E. Steiner, *Angew. Chem.* **2002**, *114*, 1628; *Angew. Chem. Int. Ed.* **2002**, *41*, 1558; b) P. W. Fowler, R. W. A. Havenith, L. W. Jenneskens, A. Soncini, E. Steiner, *Chem. Commun.* **2001**, 2386; c) R. W. A. Havenith, P. W. Fowler, L. W. Jenneskens, *Org. Lett.* **2006**, *8*, 1255.
- [14] G. R. Shelton, D. A. Hrovat, H. Wei, W. T. Borden, *J. Am. Chem. Soc.* **2006**, *128*, 12020.
- [15] T. Nishinaga, T. Uto, K. Komatsu, *Org. Lett.* **2004**, *6*, 4611.
- [16] K. Komatsu, T. Nishinaga, S. Aonuma, C. Hirosawa, K. Takeuchi, H. J. Lindner, J. Richter, *Tetrahedron Lett.* **1991**, *32*, 676.
- [17] H.-B. Bürgi, K. K. Baldridge, K. Hardcastle, N. L. Frank, P. Gantzel, J. S. Siegel, J. Ziller, *Angew. Chem.* **1995**, *107*, 1575; *Angew. Chem. Int. Ed. Engl.* **1995**, *34*, 1454.
- [18] P. v. R. Schleyer, C. Maerker, A. Dransfeld, H. Jiao, N. v. E. Hommes, *J. Am. Chem. Soc.* **1996**, *118*, 6317.
- [19] a) K. Komatsu, *Bull. Chem. Soc. Jpn.* **2001**, *74*, 407; b) K. Komatsu, T. Nishinaga, *Synlett* **2005**, 187.
- [20] K. Komatsu, S. Aonuma, Y. Jinbu, R. Tsuji, C. Hirosawa, K. Takeuchi, *J. Org. Chem.* **1991**, *56*, 195.
- [21] T. Nishinaga, T. Kawamura, K. Komatsu, *J. Org. Chem.* **1997**, *62*, 5354.
- [22] E. L. Clennan, K. Matsuno, *J. Org. Chem.* **1987**, *52*, 3483.
- [23] F. T. Bond, L. Scerbo, *Tetrahedron Lett.* **1968**, 2789.
- [24] L. Schwager, P. Vogel, *Helv. Chim. Acta* **1980**, *63*, 1176.
- [25] The same method was applied for adding artificial strain to benzene and COT nuclei; see a) A. Stanger, *J. Am. Chem. Soc.* **1991**, *113*, 8277; b) R. W. A. Havenith, L. W. Jenneskens, P. W. Fowler, *Chem. Phys. Lett.* **2003**, *367*, 468.
- [26] E. Steiner, P. W. Fowler, *Chem. Commun.* **2001**, 2220.
- [27] A. Ayalon, A. Sygula, P.-C. Cheng, M. Rabinovitz, P. W. Rabideau, L. T. Scott, *Science* **1994**, *265*, 1065.
- [28] N. L. Frank, J. S. Siegel, in *Advances in Theoretically Interesting Molecules, Vol. 3* (Ed.: R. Thummel), JAI Press, New York, **1995**, pp. 209.
- [29] The large bond alternation can also be well reproduced ( $R_{\text{endo}} = 1.440 \text{ \AA}$ ,  $R_{\text{exo}} = 1.364 \text{ \AA}$ ) by the DFT calculations at the B3LYP/6-31G(d) level.
- [30] C. F. Wilcox, Jr., R. Gleiter, *J. Org. Chem.* **1989**, *54*, 2688.
- [31] M. Magon, G. Schröder, *Liebigs Ann. Chem.* **1978**, 1379.
- [32] D. L. Mohler, K. P. C. Vollhardt, S. Wolff, *Angew. Chem.* **1995**, *107*, 601; *Angew. Chem. Int. Ed. Engl.* **1995**, *34*, 563.
- [33] A. G. Anastassiou, E. Reichmanis, *J. Org. Chem.* **1973**, *38*, 2421.
- [34] R. W. Murray, M. Singh, N. P. Rath, *Tetrahedron Lett.* **1998**, *39*, 2899.
- [35] M. J. Frisch et al., *Gaussian 98*, revision A.5, Gaussian, Inc., Pittsburgh, PA, **1998**.
- [36] CCDC-650073, CCDC-650074, CCDC-650075, and CCDC-650076 contain the supplementary crystallographic data. These data can be obtained free of charge from The Cambridge Crystallographic Data Centre via [www.ccdc.cam.ac.uk/data\\_request/cif](http://www.ccdc.cam.ac.uk/data_request/cif). The CH-COSY spectrum of **2**<sup>2-</sup>, <sup>1</sup>H and <sup>13</sup>C NMR spectra, and Cartesian coordinates of the optimized structures for all the compounds in this study are available in the Supporting Information.

Received: September 6, 2007

Revised: October 16, 2007

Published online: December 14, 2007